EVALUATION OF STEEL REINFORCEMENT CORROSION
IN CONCRETE DRAINAGE CULVERTS

M.A. Pech-Canul* and A.A. Sagüés
Dept. of Civil and Environmental Engineering
University of South Florida, Tampa, Fl. 33620

ABSTRACT

In an investigation in progress, reinforced concrete test specimens cut from two different sources of concrete culvert pipe were tested under cyclic saltwater ponding and under constant exposure to seawater. The specimens were electrochemically monitored over 700 days (cyclic test) and 400 days constant exposure for evidence of corrosion initiation and measurement of resulting corrosion rates. Corrosion initiation took place after a few months of exposure in the cyclic ponding tests. The corrosion was localized and developed at regions where the concrete cover was lowest (but still within a range consistent with manufacturing practice). Corrosion rates after initiation in the affected spots were estimated to be sufficient to cause concrete cover deterioration after a few years. No corrosion initiation took place after 400 days of continuous exposure to simulated seawater. Near-surface chloride concentrations were much higher in the concrete exposed to cyclic ponding than in that continuously exposed to salt water. Within each exposure regime, the concrete containing fly ash developed a higher near-surface chloride content than the OPC. The apparent chloride diffusivity of the OPC concrete was greater than that of the concrete containing fly ash, even though the reported total binder content of the OPC concrete was higher. The average estimated threshold chloride concentration under cyclic ponding conditions for fly ash containing concrete was ~ 0.6% of binder content. For OPC concrete it was ~ 0.34% of binder content, but the latter value may be underestimated since stable corrosion initiation in the OPC concrete was not observed.

Keywords: concrete, culverts, chlorides, ponding, fly ash, durability.

INTRODUCTION

Design service life requirements for reinforced concrete highway culverts commonly approach 100 years[1]. However, durability estimates made with current guidelines for culvert material selection are subject to uncertainty. To improve the present methods for performance prediction several reinforced concrete performance parameters need to be determined more accurately. Of particular interest is the case of culverts exposed to seawater or dilutions thereof, since under those conditions useable service life may be significantly reduced.

Reinforced concrete deteriorates because of chemical degradation of the concrete itself (due to the presence of acidity and sulfates in the soil) and because of corrosion of the reinforcement. The latter process involves first an initiation period (t_{cr}), in which the penetration of chloride ions through the concrete cover ending with depassivation of the steel surface takes place. A propagation stage follows in which the steel corrodes until the concrete cover is cracked or other externally evident damage occurs[2]. It is of importance to determine the ability of present-day concrete formulations used in culverts to resist chloride ion penetration.

Current methods for service lifetime prediction of chloride exposed reinforced concrete structures assume the existence of a critical or threshold chloride concentration (C_{cr}) below which active corrosion is unlikely to occur. This threshold limit is generally expressed in terms of total chloride (i.e. 'bound'+'free') where 'free chlorides' are dissolved in the pore water and 'bound chlorides' are either chemically or physically absorbed by the concrete. Any t_{cr} prediction is based on the speed of chloride accumulation at the rebar surface, and computation of the time necessary to achieve a concentration equal to C_{cr}. A simplified forecast method consists of assuming planar geometry with a concrete surface that has a constant chloride concentration (C_s). Chloride ion transport through the concrete cover is then assumed to take place by homogeneous diffusion with time-invariant apparent diffusivity (D_{app}).

Two factors which are of importance for service life prediction are the concrete composition and the type of environment (e.g. intermittent or continuous contact with brackish water). The partial replacement of cement with fly ash, for instance, has been reported to reduce the threshold chloride concentration[3] but also, more markedly, the value of the apparent diffusion coefficient[4-6]. The environment has an important effect on the surface chloride concentrations, since at regions where wetting and drying cycles occur, a progressive evaporative buildup of chlorides[6] takes place. Some researchers have suggested that C_{cr} is also affected by the environmental conditions, for example being lower in atmospherically exposed concrete than in permanently water saturated concrete.[7,8]

In this study two types of concrete culverts (made with ordinary portland cement (OPC) and OPC blended with fly ash) were tested. The issue of environmental effect was addressed by using two types of ponding tests with chloride-rich water solutions. The specimens used for this laboratory investigation were cut from actual production pipes and had a range of concrete cover thicknesses, which offered an opportunity to examine the effect of dimensional variability on corrosion initiation times. The findings presented here are the first results of an ongoing investigation.

EXPERIMENTAL

Reinforced concrete drainage pipes 38 cm (15 in) inner diameter, from two different manufacturers and complying with ASTM C76-90, were used in this study. Each maker used different concrete mix proportions, given in Table 1. The two were identified as "O" and "F" in this paper. As reported by the manufacturers, the pipes of types O and F were made by the dry cast and by the packerhead methods, respectively. Type O pipes were demolded right after casting, kept indoors 24 h and then moved outdoors for air curing; type F pipes were also demolded right after casting, kept indoors overnight, and then moved outdoors for air curing. The reinforcing cages of concrete pipes type O and F were made with 4.76 mm (3/16 in) and 6.35 mm (1/4 in) diameter steel wire, respectively. Both types of pipes had a wall thickness of 6.35 cm (2½ in). One pipe of each type was cut into 40.6 cm (16 in) long rings to obtain laboratory specimens. The rings were cut from the central bodies of the pipes avoiding end sections. Each ring was then cut into quadrants in order to get at least one longitudinal steel wire near the center of the quadrant. The resulting specimens (Figure 1) were arc-shaped, 41 cm (16 in) long and 36 cm (14 in) outer cord.

Small spots of the inner surface of the specimens obtained from both types of pipes were chipped off with a chisel and phenolphthalein solution was mist-sprayed over the newly broken surfaces. Then carbonation depths were measured at different points of the inner surface. The average carbonation depths were ~4 mm and ~ 1 mm for type F and type O specimens respectively. These tests were performed shortly before the beginning of the test exposures described below.

Twelve specimens (six from each pipe type) were prepared by attaching acrylic ponding dams to the concave side with a clear silicone adhesive. The dam footprint was 28 cm x 15 cm (11.1 in x 6.1 in). The remaining concave surface and cut edges of the specimens were coated with an epoxy sealer paint. Each specimen had a brass screw tapped into the end of one longitudinal wire to serve as the working electrode connection. The wire cage was electrically continuous. Six specimens (3 of type O and 3 of type F), hereafter named "set A", were exposed to intermittent ponding with 3% NaCl solution to allow for a wetting-evaporation cycle regime. Each exposure cycle consisted of 2 weeks ponding followed by two weeks drying. During each cycle a new ponding solution with the same concentration was used, filling the dam to a height of 38 mm (1.5 in). The other six specimens, hereafter named "set B", were ponded continuously during 8 months with distilled water, and with simulated seawater (ASTM D1141-90) thereafter. Each specimen of set B was normally enclosed in a plastic bag, and distilled water was periodically sprayed inside in order to maintain a high humidity environment. Each specimen was named with a 3-character code as exemplified by F1A, which stands for specimen number one of concrete pipe type F, used in intermittent ponding (set A). The laboratory conditions were ~ 60% R.H. and 22 ° C.

For determination of chloride concentration profiles, selected specimens were drilled at increasing depths from the concave surface and the powders were analyzed for total chloride ion content by acid digestion, according to the standard procedure FM 6-656 established by the Florida Department of Transportation (FDOT).[9]

Distributions of concrete cover depth (cc) for all twelve specimens were obtained by measuring the minimum distance between the specimen inner surface and each wire cross

section exposed in the cut sides. Each specimen yielded about 12 cc values, which were then examined statistically.

The results presented in this paper correspond to a total exposure time of 756 days for set A (approximately 25 cycles) and 390 days of continuous salt water ponding for set B. Continuing test exposures are in progress. Parameters monitored during the corresponding exposure times, included open circuit potential of the wire (E_{oc}), polarization resistance (R_p) and concrete resistivity (ρ).

For the electrochemical tests on each specimen, a saturated calomel electrode (SCE) was placed in one corner of the acrylic dam. A 7.6 cm (3 in) by 12.7 cm (5 in) activated titanium mesh[10] was temporarily placed at the bottom of the dam and used as the counter electrode. All electrochemical tests were conducted when the ponds were full. Conventional polarization resistance tests were conducted by varying the potential (starting from E_{oc}) in the negative direction, at a scan rate of 0.05 mV s^{-1}. Surface-normalized apparent polarization resistance values were obtained by multiplying the apparent polarization resistance ($R_{p,app}$) by the nominal specimen exposed metal area. This area was considered to be that of the reinforcing cage section defined by the ponding dam footprint. The values used were 237 cm^2 (36.8 in^2) for specimens type F and 178 cm^2 (27.6 in^2) for specimens type O. Conversion to nominal corrosion current densities (i_{corr}), after compensation for IR drop effects, was made by using a Stern-Geary constant B=26 mV.[11]

Electrical resistance R was measured between the wire and the titanium mesh (during the wet cycle for set A) using a Model 400 Nilsson soil resistivity meter. R was then converted to a concrete resistivity value ρ, by multiplying it by a geometrical cell constant (C_k) which was determined using the heat transfer analogy for a row of tubes at equal depth in a semi-infinite solid.[12] A Value of C_k was calculated for each specimen, taking into account the diameter of the steel wire, the average concrete cover depth and the size of the dam footprint. The typical cell constant calculated by this method was within 87-91% of the value calculated for two parallel plates.

The data of E_{oc}, i_{corr}, and ρ for set A presented in this paper are from measurements normally made near the end of each wet cycle. Measurements for set B were made approximately every 30 days.

RESULTS

Figures 2 (a) and 2 (b) show plots of the cumulative % of exposed wire cross sections in the cut edges of the specimens versus clear concrete cover thickness, for set A and set B, respectively. The average cover for type O specimens was generally greater than for type F. One exception was specimen O2A for which approximately 50% of the spots examined presented values of cc in the same range as specimens F1A and F3A for the same cumulative level. The lowest values of cc (about 12 mm (~ 0.5 in)) were found in specimens F2A, F4B and F5B. As expected, in both types of concrete pipes (O and F) the longitudinal reinforcement was closer to the inner surface of the pipe than the transversal (hoop) reinforcement. Figure 3 confirms that the lower values of cc were normally found in the spots corresponding to longitudinal wires, although in some cases, probably due to tight winding of the hoop wire, the

opposite was observed. In Figure 4 the cumulative frequency distributions of concrete covers for specimens F1A and F2A are plotted again, but using different symbols for wire cross sections examined in different cut edges of the specimens. It is clear that the cover was not uniform around the pipe perimeter, showing some degree of eccentricity in the placement of the reinforcing cage within the walls of the concrete pipe.

The chloride concentration profiles for selected specimens of each pipe type are presented in Figure 5. It can be seen that for the concrete containing fly ash (F1A) the chloride profile showed a maximum about 6 mm inside the concrete surface, slightly ahead of the carbonation front (located at 4 mm from the surface). Such an effect has been observed by other authors.[2,13-15] It has been proposed that in carbonated layers both the porosity[16] and the chloride binding ability[14,15] of the concrete are reduced, thus decreasing the total chloride content compared to the amount present in uncarbonated concrete exposed to the same medium. Specimen O2A (containing only OPC) showed lower chloride concentrations in the region of 6-24 mm from the concrete surface than those observed for F1A. A similar behavior for fly ash versus OPC concretes was observed by other authors.[17,18] For specimen O2A the carbonation depth was only ~1 mm and did not seem to have a pronounced effect on the observed chloride concentration profile. Figure 5(b) shows the chloride concentration profiles for specimens F5B and O4B of set B, after 390 days of continuous immersion in simulated seawater. The high chloride uptake near the surface for the fly ash containing specimen and the maximum just ahead of the carbonation front noted for set A were also observed for set B.

Figure 6 (a) shows the trends in open circuit potentials measured near the end of each wet cycle, for the specimens of set A. The initial potential for all of them was about −150 mV vs CSE. The E_{oc} values remained high throughout the test period only for specimens O1A, O3A and F3A. The potential of specimen O2A experienced a drop to −360 mV vs CSE as early as about 50-90 days, but oscillated between low and high values afterwards. For specimens F2A and F1A a more permanent potential drop occurred at about 120 days and 340 days, respectively. The E_{oc} values for these two specimens tended to attain, at the end of the test period, a roughly constant value near −400 mV vs CSE. The plots of E_{oc} versus exposure time for specimens of set B, given in Figure 6 (b) show that for "O" specimens the potentials remained high throughout the 390 days of exposure to simulated sea water. The E_{oc} values of the "F" specimens tended to be more negative, and after 390 days they were in the range −200 to −320 mV vs CSE. A sudden drop in potential was not observed for any of these permanently wet specimens.

Figures 7 (a) and (b) show equipotential contour maps for specimens F1A and F2A, plotted on a suitably scaled plan view of the dam footprint. The potentials were measured placing a SCE sequentially over points of a grid (1/2 in centers) traced on the specimens inner surface. The measurements were made after 9 days drying during the 21st dry cycle. It can be observed that, although the maximum potential difference within each specimen does not exceed 75 mV, there are regions with potentials less than −300 mV vs SCE. The dashed lines in both figures represent the approximate locations of the wires under the ponding area. The data in Figure 4 suggest that for specimen F1A the part of the reinforcing cage on the right hand side of the dam area was closer to the specimen inner surface. Figure 7 (a) shows that it was precisely in that region where the potentials were more negative. A similar observation can be done for specimen F2A, but with the region with closest distance to the inner surface being on the left hand side of the dam area.

Apparent corrosion current densities (i_{corr}) for the specimens of sets A and B are presented, respectively, in Figures 8 (a) and (b) as a function of exposure time. In agreement with indications from the trends in E_{oc}, three specimens (F3A, O1A and O3A) of set A had very low apparent corrosion rates suggesting that they were still under passive conditions at the end of the test period. For specimens O2A, F2A and F1A the time for the onset of active corrosion, inferred from the open circuit potential trends, seems to be consistent with the time when i_{corr} reached values of 0.05-0.15 μA cm^{-2}. After two years of exposure the values of i_{corr} for F1A and F2A were roughly between 0.1 and 0.3 μA cm^{-2}, thus suggesting a low corrosion rate. For set B, the i_{corr} values were between 0.01 and 0.1 μA cm^{-2} for type F culverts and around 0.01μA cm^{-2} for type O specimens.

Figures 9 (a) and 9(b) show the evolution of concrete resistivity as a function of exposure time for set A and set B, respectively. For specimens of set A, the concrete in the type F culvert had initially resistivities four times higher than that of the type O culverts. The value of ρ seemed to increase with exposure time for both types of concrete and at the end of the test period, values in the order of 30-70 kΩ cm had been reached. For set B the resistivities were in the order of 30 kΩ cm for type O and 100 kΩ cm for type F, and did not change significantly throughout the exposure to simulated sea water.

DISCUSSION

Based on the chloride concentration profiles and on the observed times to active corrosion initiation for specimens O2A, F2A and F1A an attempt was made to obtain preliminary estimates of durability design parameters. These estimates will be revised as additional results develop from continuing exposure testing.

Corrosion initiation period

Set A (cyclic ponding in 3% NaCl). The chloride concentration profiles in Figure 5 (a) were obtained after 756 days of intermittent exposure to sodium chloride solutions. Nominal values of the surface concentration C_s and the apparent diffusion coefficient D_{app} corresponding to this exposure period were obtained for specimens F1A and O2A by fitting the data to the solution of a one dimensional simple diffusion model with zero initial bulk concentration and constant surface concentration, represented by the following equation, in which x is the distance from the surface and t is the time:

$$C(x, t) = C_s \left(1 - erf\left(\frac{x}{2\sqrt{D_{app}t}} \right) \right)$$ (1)

For specimen F1A the analysis was carried out using only points beyond the carbonation front (located at 4 mm from the surface) and it was assumed, as a working approximation, that the position of constant concentration (x=0) was located 4 mm from the concrete surface. The values of C_s and D_{app} obtained by this method are presented in Table 2. While application of Eq. (1) to the data in Figure 5 involves numerous simplifications, some tentative observations may be made. The surface concentrations estimates appear to be in keeping with those commonly obtained in ponding regimes of this type.[18] The value of D_{app} for the type F

specimens (on the order of values typically obtained for somewhat permeable concretes[19]) is consistent with the reported low cementitious factor of the concrete used (only 295 kg/m^3), which does not appear to have been compensated by the beneficial pozzolanic replacement and the small water to binder ratio. The type O specimens had concrete with a reported greater binder content (356 kg/m^3) and even lower water to binder ratio than those of type F. Although concrete in type O specimens did not include fly ash, it is surprising in view of the richer proportioning that the chloride profile was significantly broader (and consequently D_{app} was significantly greater) than that of the type F specimens. The absolute values of D_{app} for both types F and O seem to be higher than those typically found elsewhere[20] for concretes with wet resistivity values similar to those reported for each type in Figure 9. Additional results and more sophisticated profile modelling will be required to examine this issue.

The potential maps in Figure 7 show that for specimen F1A the more negative potentials are in the right hand side region of the grid. According to the distribution of cover depths (Figure 4) the longitudinal steel wire in that region was the closest to the inner surface, with a minimum cover depth cc_{min}=19 mm. Similarly for specimen F2A, the more negative potentials corresponded to the longitudinal wire in the left hand side of the dam area, and cc_{min} was found to be 16 mm. For specimen O2A a value of cc_{min}=17 mm was determined using only the cover depth distribution data.

To obtain estimates of the chloride threshold level for specimens F1A and O2A, their concentration profiles were scaled to the observed times for initiation of corrosion activity (340 days for specimen F1A and 80 days for specimen O2A) assuming that the value of x for any given concentration is proportional to the square root of time.[21] Such relationship stems from the simplifying assumptions for Eq.(1) and must be viewed only as a means to obtain a rough estimate. The values of C_{cr} were determined using smoothed concentration profiles considering C_{cr}=C(x=cc_{min}, t_{cr}). Based on the assumption that the chloride penetration pattern might be similar for specimens cut from the same concrete pipe and exposed to similar conditions, the profile for specimen F1A was also scaled to 120 days to estimate C_{cr} for specimen F2A. The results are presented in Table 3. The estimates for the two type F specimens are different, reflecting possible actual variability but also the simplified character of the assumptions made. The values obtained for both types of specimens are nevertheless not unreasonable compared with typically assumed values for the concentration threshold.[22] The specimens showing indications of corrosion initiation during the test period were among those with the lowest minimum cover values. Projected times to corrosion initiation (t_{cr}) can be calculated for the remaining specimens by application of Eq. (2), which follows from Eq. (1),

$$ t_{cr} = \left(\frac{cc_{min}^2}{4D_{app}} \right) \left(erfinv\left(1 - \frac{C_{cr}}{C_s} \right) \right)^{-2} \tag{2} $$

as well as using the results from Table 2, the average experimental C_{cr} estimates in Table 3, and the corresponding minimum concrete covers of each specimen. The projected initiation time for specimen F3A is about 680 days, which is near the present time. For specimens O3A and O1A t_{cr} is about 310 days and 360 days respectively. This result suggests that C_{cr} for type O specimens might be underestimated. Taking into account the oscillating trend in E_{oc} and the low values of apparent corrosion current density (~0.05 μA cm^{-2}), it is possible that specimen O2A had not actually reached the initiation period end, if it were defined as the moment of permanent passivity loss. Although i_{corr} for specimen O2A is very close to i_{corr} for specimen

F1A at the end of the test period the actual corrosion rate for specimen F1A (and also for F2A) might be higher due to localized corrosion, as evidenced from the potential mapping (Figure 7). The validity of these projections and a better insight of the corrosion behavior for type O specimens will be established by continued testing.

Set B (continuous ponding in simulated seawater). The chloride concentration profiles in Figure 5 (b) were obtained for specimens F5B and O4B after 390 days of continuous exposure to simulated seawater. From them, nominal values of C_s and D_{app} were obtained by fitting the data as indicated earlier, and they are presented in Table 2. The C_s values are lower than those in the intermittent ponding regime, as expected since in these specimens there is no evaporative enrichment of the solution at the surface. There was no corrosion initiation in any of the continuously ponded specimens in the test period, which is consistent with calculations using the minimum covers measured, the values of C_s in Table 2, and assuming that the C_{cr} values for the B specimens are similar to the average for each concrete type obtained for the A series. The earliest projected times for corrosion initiation under those assumptions are on the order of 1.5 years for type F and 4.5 years for type O specimens. Much longer initiation time estimates could result if higher nominal C_{cr} values were used (as those proposed for permanent immersion conditions, in Ref. 8). Continuing testing is in progress to elucidate the validity of these projections.

Corrosion Propagation Period

Corrosion rate information is available so far only for the intermittent ponding experiments. The nominal corrosion rates shown in Figure 8 are very small even for specimens that had entered an apparently well defined active corrosion period. However, the corrosion was very likely localized to small portions of the reinforcement assembly, as evidenced by the potential maps in Figure 7. Preliminary examination of the potential maps based on modeling of corrosion distribution in concrete[23] suggests that the area of active corrosion in specimens F1A and F2A was about one order of magnitude smaller than the total steel area of each specimen. Therefore (keeping in mind the numerous sources of error in corrosion rate estimation from polarization measurements in concrete[24-26]), corrosion current densities in the corroding spots of specimens F1A and F2A may be estimated to be on the order of 1μA/cm^2, or about 10 μm/year. If corrosion rates of this magnitudes were sustained after corrosion initiation, cracking of the concrete cover could be expected after a few years of corrosion.[27-28] The constant immersion specimens are expected to experience lower average corrosion rates after corrosion initiation because of the lower oxygen diffusivity in water-saturated concrete[2]. However, if the corrosion is localized as in the series A tests, there may be enough corrosion macrocell coupling over extended distances to maintain a comparatively large overall cathodic reaction rate and correspondingly high local corrosion rates.

Overall Durability Considerations

The limited results available to date suggest that in very aggressive saltwater service (wet-dry cycling) localized corrosion in regular production culvert pipes can initiate in as little as a few months, and propagate at rates sufficient to compromise cover integrity after a few years after initiation. The development of corrosion initiation over the entire culvert body may be anticipated from the cover distribution curves shown in Figures 2 to 4; a quantitative treatment based on those distributions is planned after mature corrosion patterns develop in more of the

test specimens in the present test sequence. Nevertheless, it appears that the prognosis for very long durability (e.g. 100 years) under frequent wet-dry salt water exposure is poor.

The results also suggest that continuous immersion in seawater represents a less severe corrosion initiation regime, based on the lower levels of effective surface concentration and on the lack of corrosion initiation events to date, which may be an indication also of higher chloride concentration thresholds in the permanently wet concrete. Results from an extended test sequence are needed before attempting to evaluate the long-term durability prognosis under this service condition.

CONCLUSIONS

1) Corrosion initiation in regular production culvert pipe exposed to cyclic saltwater ponding-drying took place in as little as a few months. The corrosion was localized and developed at regions where the concrete cover was lowest (but still within a range consistent with manufacturing practice). Corrosion rates after initiation in the affected spots were estimated to be sufficient to cause concrete cover deterioration after a few years.

2) No corrosion initiation took place after 400 days of continuous exposure to simulated seawater.

3) Near-surface chloride concentrations were much higher in the concrete exposed to cyclic ponding than in that continuously exposed to salt water. Within each exposure regime, the concrete containing fly ash developed a higher near-surface chloride content than the OPC. The apparent chloride diffusivity of the OPC concrete was greater than that of the concrete containing fly ash, even though the reported total binder content of the OPC concrete was higher.

4) The average estimated threshold chloride concentration under cyclic ponding conditions for fly ash containing concrete was ~ 0.6% of binder content. For OPC concrete it was ~ 0.34% of binder content, but the latter value may be underestimated since stable corrosion initiation in the OPC concrete was not observed.

ACKNOWLEDGEMENT

REFERENCES

1. W.D. Cerlanek, R.G. Powers, "Drainage Culvert Service Life Performance and Estimation", State of Florida Department of Transportation Report No. 93-4A, April, 1993.

2. K. Tuuti, " Corrosion of Steel in Concrete" (Stockholm, Swed: Swedish Cement and Concrete Research Institute, 1982).

3. M. Thomas, Cem. Concr. Res. 26,4 (1996): p. 515.

4. R.K. Dhir, E.A. Byars, Mag. of Concr. Res. 45,162 (1993): p.1.

5. P.B. Bamforth, "Concrete Clasiffication for R.C. Structures Exposed to Marine and Other Salt-Laden Environments", presented at Structural Faults And Repairs, Edinburgh, Scotland, 1993.

6. P.B. Bamforth, "Factors Influencing Chloride Ingress Into Marine Structures", in Concrete 2000, eds. R.K. Dhir, M.R. Jones, (London, UK : Chapman & Hall, 1993): p. 1105.

7. P.K. Mehta, P. Schiessi, M. Raupach," Performance and Durability of Concrete Systems", in Proceedings of the 9th International Congress On the Chemistry of Cement, New Delhi, India, 1992, p.571.

8. E. Poulsen, J.M. Frederiksen, L. Mejbro, "Chloride Exposed R-C structures. Chloride Ingress and Lifetime Prediction by the Hetek-Model", presented at the ASTM Workshop on Models For Predicting The Service Life and Life-Cycle Cost of Steel-Reinforced Concrete, Gaithersburg, MD, November 9-10,1998.

9. FDOT, " Florida Method of Test for Determining Low-Levels of Chloride in Concrete and Raw Materials", FM 5-516, Florida Department of Transportation, September 1994.

10. P. Castro, A.A. Sagüés, E. Moreno, L. Maldonado, J. Genescá, Corrosion 52, 8 (1996): p. 609.

11. C. Alonso, C. Andrade, Adv. Cem. Res., 1, 3 (1988): p. 155.

12. W.M. Rohsenow, J.P. Hartnett, E. N. Ganic, Handbook of Heat Transfer Fundamentals, Second ed., McGraw-Hill 1985, p. 4-165.

13. C. Arya, J.B. Newman, Proc. Instn. Civ. Engrs, Part 1, 88 (1990): p. 875.

14. C. Andrade, Advn. Cem. Bas. Mat., 6 (1997): p.39.

15. L. Tang, L-O. Nilsson, Cem. Concr. Res., 25, 4 (1995): p. 695.

16. V.G. Papadakis, M.N. Faedis, C.G. Vayenas, ACI Mat. Journal, 89, 2 (1992): p. 119.

17. P.S. Mangat, J.M. Khatib, B.T. Molloy, Cement & Concrete Composites 16 (1994): p. 73.

18. R.N. Swammy, J.C. Laiw, "Effectiveness of Suplementary Cementing Materials in Controlling Chloride Penetration in Concrete", in Proceedings of the 5th International Conference on Fly Ash, Silica Fume, Slag, and Natural Pozzolans in Concrete, ACI SP-153, vol. 2, ed. V.M. Malhotra, (Milwaukee, WI, 1995): p. 657.

19. P.B. Bamforth, "Chloride Penetration and Service Life", presented at Corrosion and Protection of Metals in Contact with Concrete- COST-509 Workshop, Sevilla, Spain, Sept. 1995.

20. N.S. Berke, M.C. Hicks, "Estimating the Life Cycle of Reinforced Concrete Decks and Marine Piles Using Laboratory Diffusion and Corrosion Data", in "Corrosion Forms and Control for Infrastructure", ASTM STP 1137,ed. V. Chacker, (Philadelphia, PA: American Society for Testing and Materials, 1992), p.207.

21. J. Crank, The mathematics of Diffusion, 2nd Edition (Oxford, UK: Oxford University Press, 1975): p. 37.

22. R.E. Weyers, B.D. Prowell, I.L. Al-Qadi, M.M. Sprinkel, M. Vorster," Concrete Bridge Protection, Repair, and Rehabilitation Relative to Reinforcement Corrosion: A Methods Application Manual", SHRP-S-360, (Washington, DC:National Research Council, 1993).

23. S.C. Kranc, A.A. Sagüés, F.J. Presuel-Moreno, " Computation and Experimental Investigation of Cathodic Protection Distribution in Reinforced Concrete Marine Piling", CORROSION 97, paper no. 231, (Houston, TX: NACE International, 1997).

24. A.A. Sagüés, S.C. Kranc, " Computer Modeling of Effect of Corrosion Macrocells on Measurement of Corrosion Rate of Reinforcing Steel in Concrete", in " Corrosion Activity of Steel Reinforced Concrete Structures", ASTM STP 1276, eds. N.S. Berke, E. Escalante, Ch.K. Nmai, D. Whiting, (West Conshohocken, PA: American Society for Testing and Materials, 1996), p.58.

25. A.A. Sagüés, S.C. Kranc, Corrosion 48, 8 (1992): p. 624.

26. A.A. Sagüés, S.C. Kranc, E.I. Moreno, Corrosion 54, 1 (1998): p. 20.

27. C. Andrade, C. Alonso, "Progress on Design and Residual Life Calculation with Regard to Rebar Corrosion of Reinforced Concrete", in " Corrosion Activity of Steel Reinforced Concrete Structures", ASTM STP 1276, eds. N.S. Berke, E. Escalante, Ch.K. Nmai, D. Whiting, (West Conshohocken, PA: American Society for Testing and Materials, 1996), p.23.

28. A.A. Torres-Acosta, A.A. Sagüés, " Concrete Cover Cracking and Corrosion Expansion of Embedded Reinforcing Steel", in "Rehabilitation of Corrosion Damaged Infrastructure, Chapter IV: Modelling, Methods, Techniques and Technologies", eds. P. Castro, O. Troconis, C. Andrade, (Yuc, MX: 1998): p. 215.

TABLE 1
Mix proportions (as reported by each manufacturer)

Mix ref.	Cement	Cement content (C)	Fly ash content (FA)	w/(C+FA)
		$(Kg\ m^{-3})$	$(Kg\ m^{-3})$	
O	OPC	356	0	0.32
F	OPC/Fly ash (type "F")	236	59	0.37

TABLE 2

Diffusion parameters obtained by regression using Eq. (1) and simplifying assumptions.

Environment type	specimen	T	C_s	D_{app}
		(days)	$(Kg\ m^{-3})$	$(cm^2\ s^{-1})$
Set A	F1A	756	14.7	2.3×10^{-8}
	O2A	756	8.9	8.5×10^{-8}
Set B	F5B	390	5.2	2.3×10^{-8}
	O4B	390	2.8	5.1×10^{-8}

TABLE 3

Estimated chloride threshold concentrations for specimens of set A

specimen	t_{cr}	C_{cr}	
	(days)	(Kg m^{-3})	% binder content
F1A	340	2.7	0.9
F2A	120	1.1	0.38
O2A	80	1.2	0.34
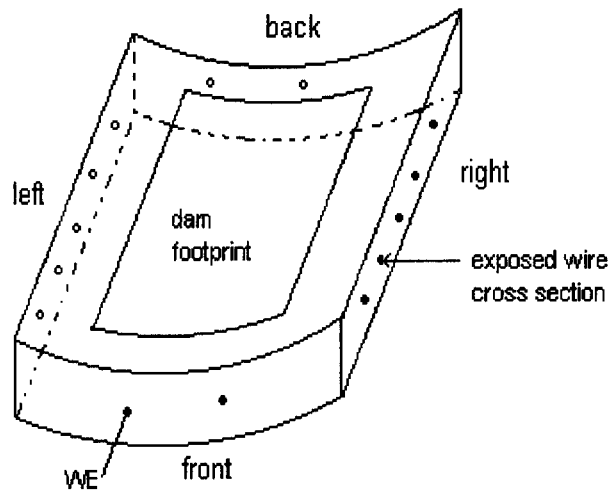
Figure 1. Sketch of the specimens used. The cut edge with the connection for the working electrode (WE) was considered to be the front of the specimen.
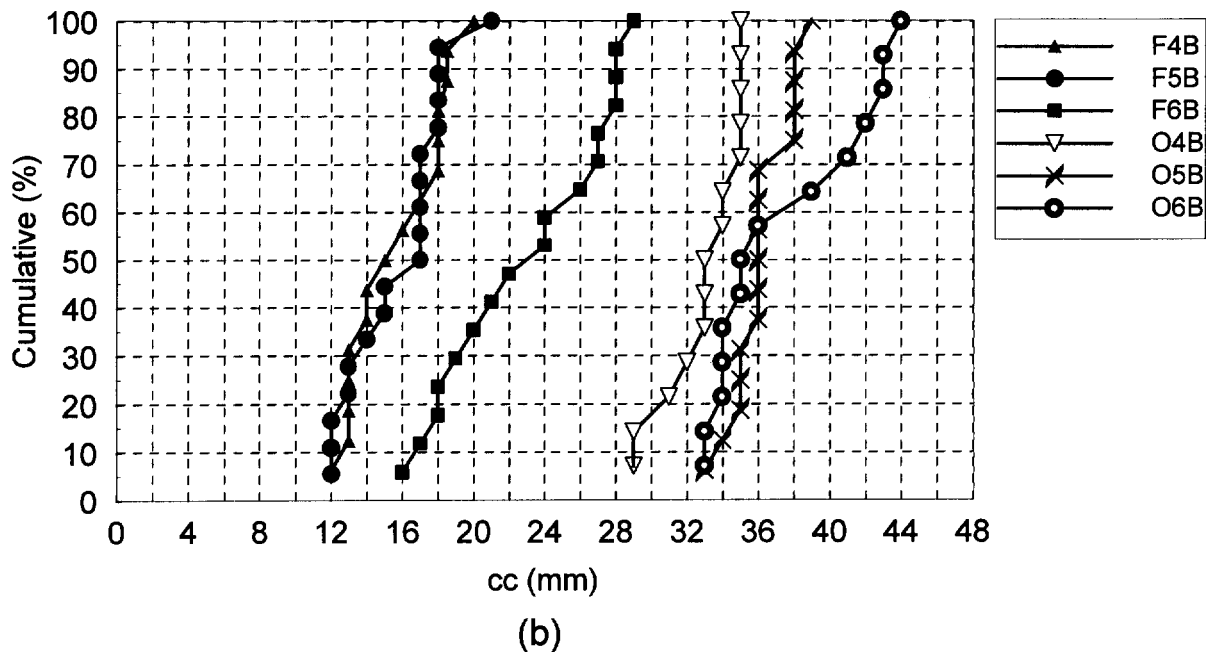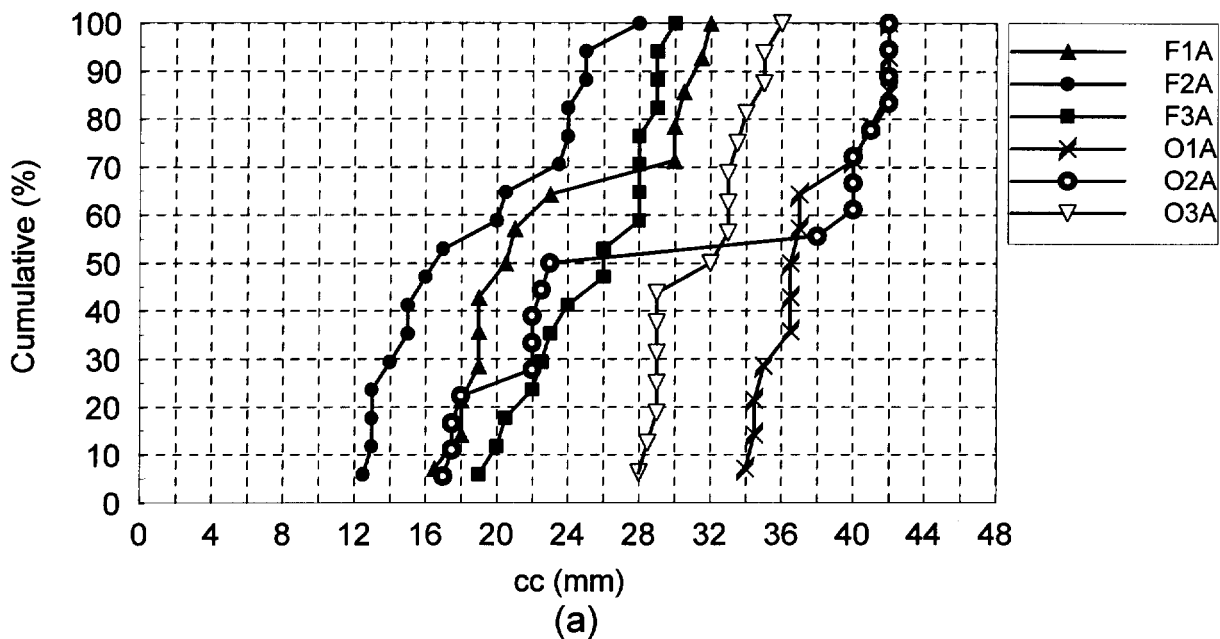
Figure 2. Cumulative percentage of steel wire cross sections examined in the cut edges *vs* concrete cover thickness (cc) for specimens corresponding to : a) set A and b) set B.
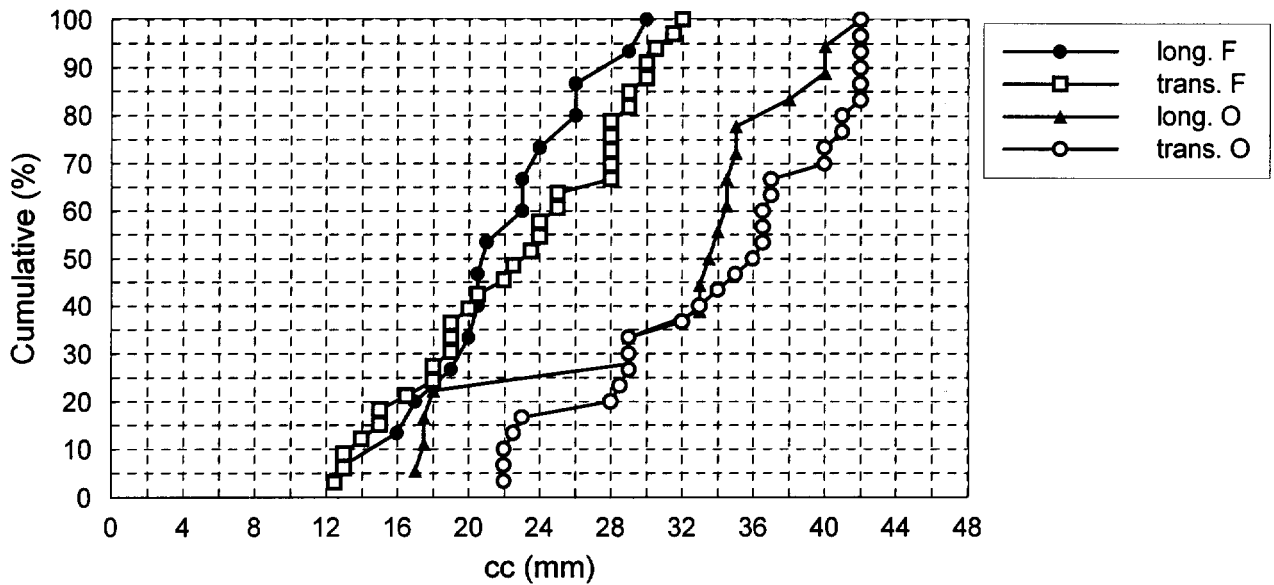
Figure 3. Distribution of concrete cover with cc values for cross sections of longitudinal and transversal wires plotted separately. Data for all six specimens of : a) set A and b) set B.
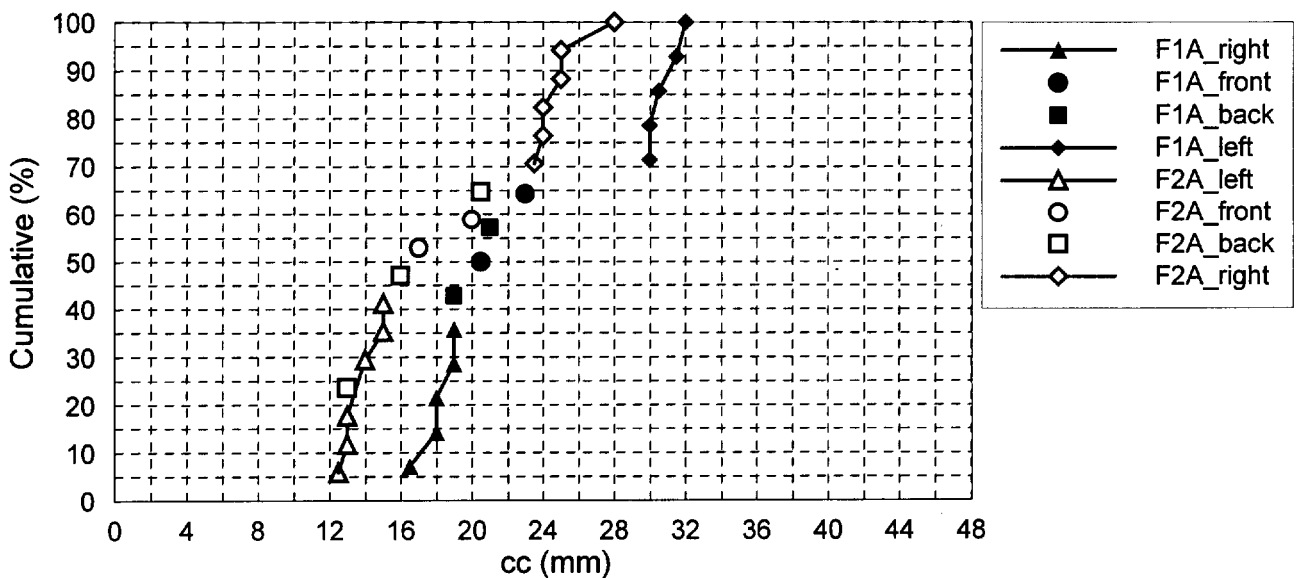
Figure 4. Distribution of concrete cover for specimens F1A and F2A, using different symbols for spots corresponding to different cut edges of the specimens, according to the convention given in Figure 1.
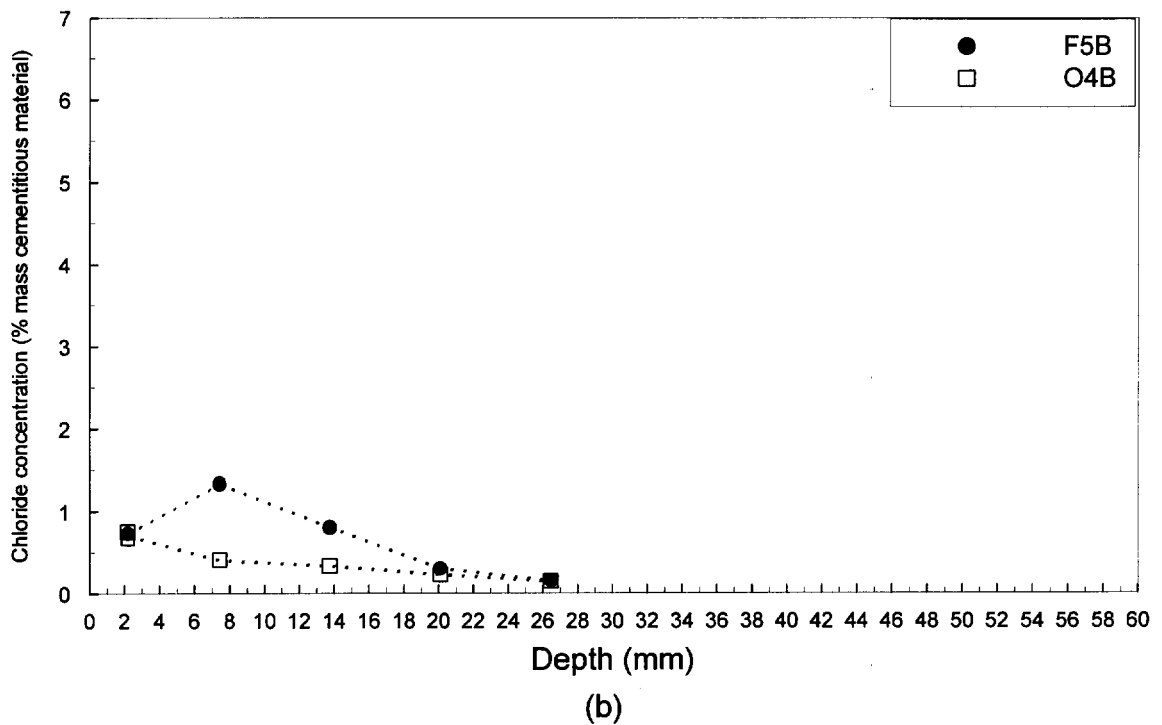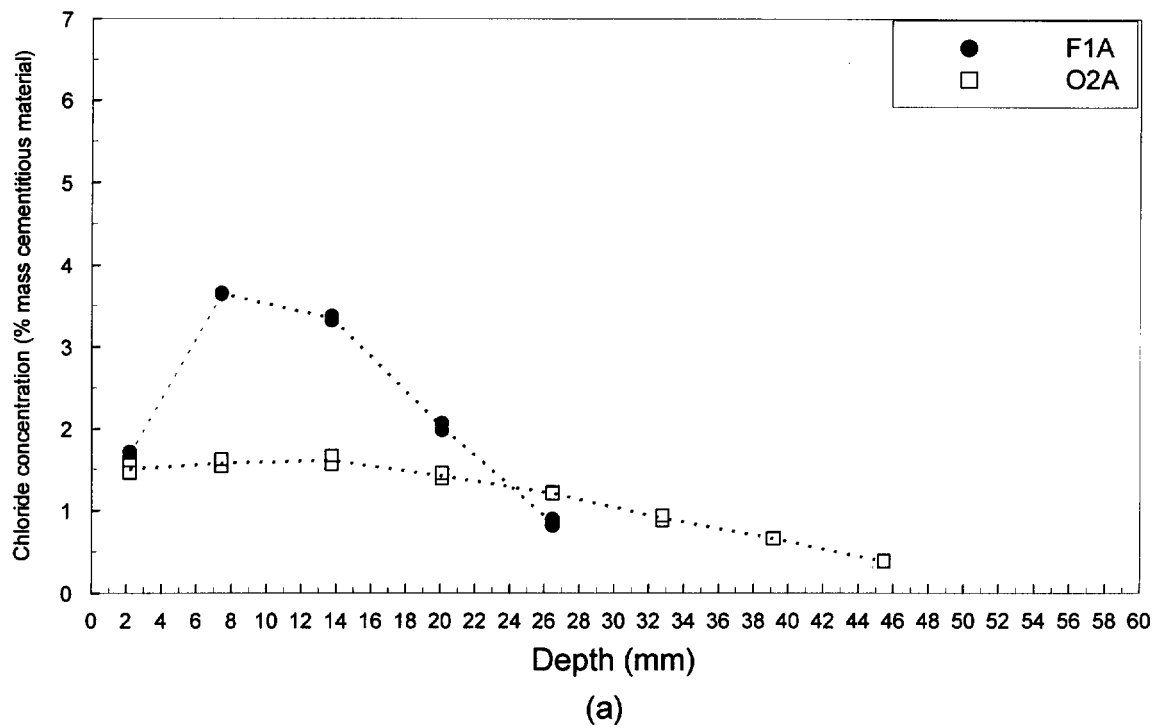
Figure 5. Chloride profiles for selected specimens of : a) set A (756 days of exposure), and b) set B (390 days of exposure). Symbols show values of duplicate tests (i.e. duplicate chloride analysis were made for concrete powder samples at each depth).
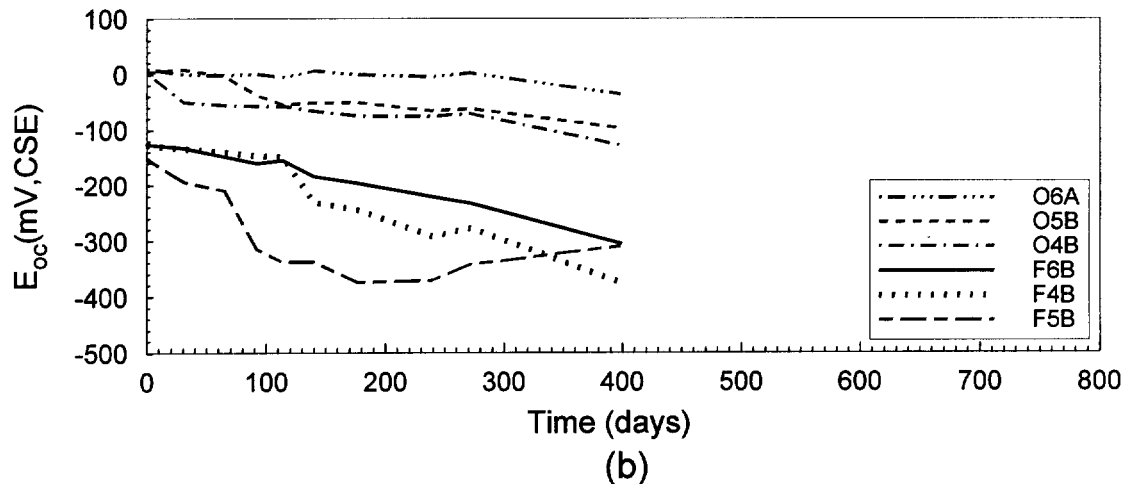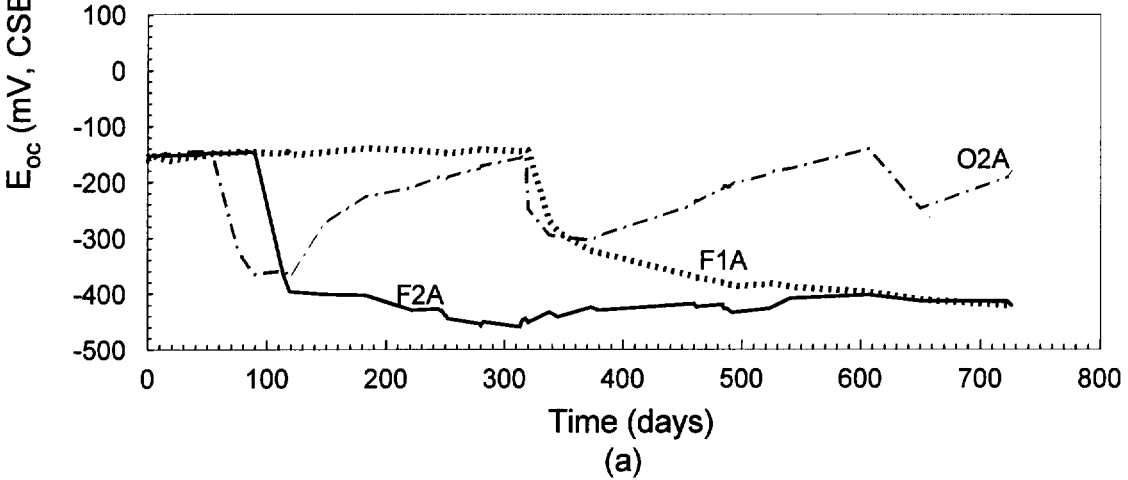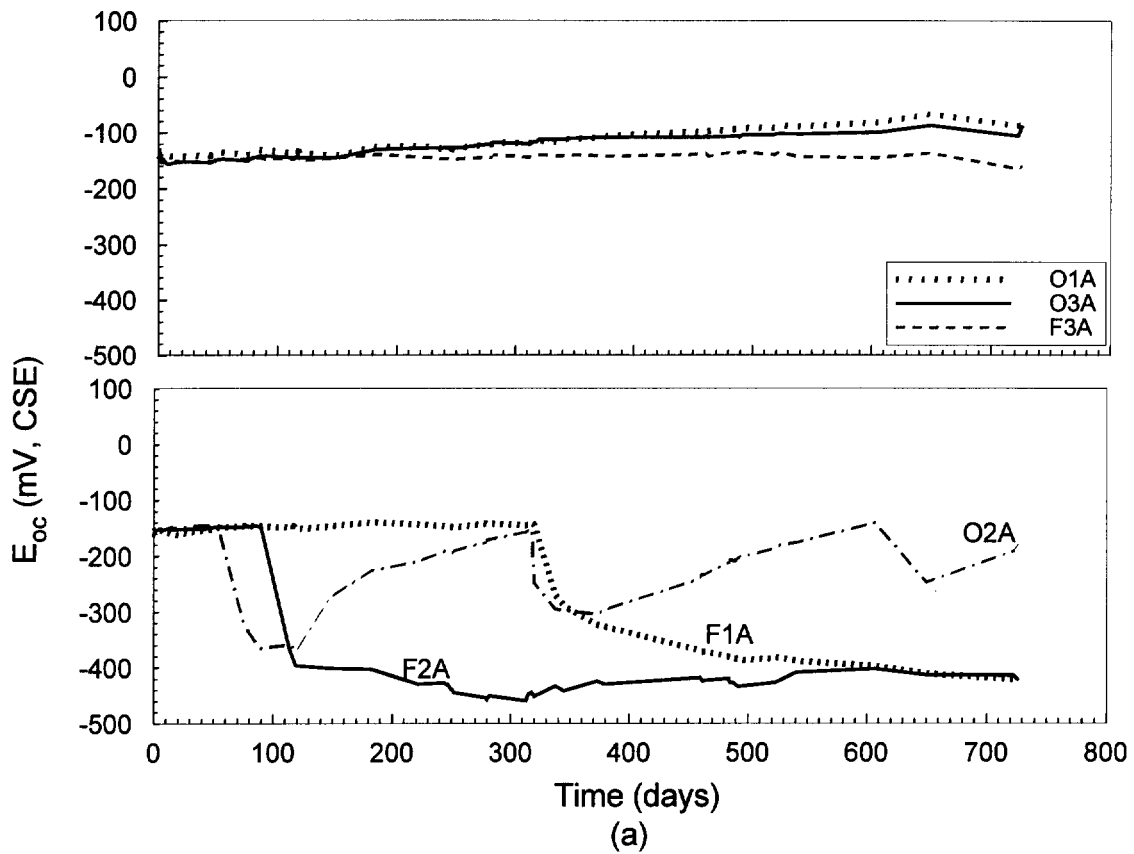
Figure 6. Open circuit potentials as a function of exposure time for specimens of :
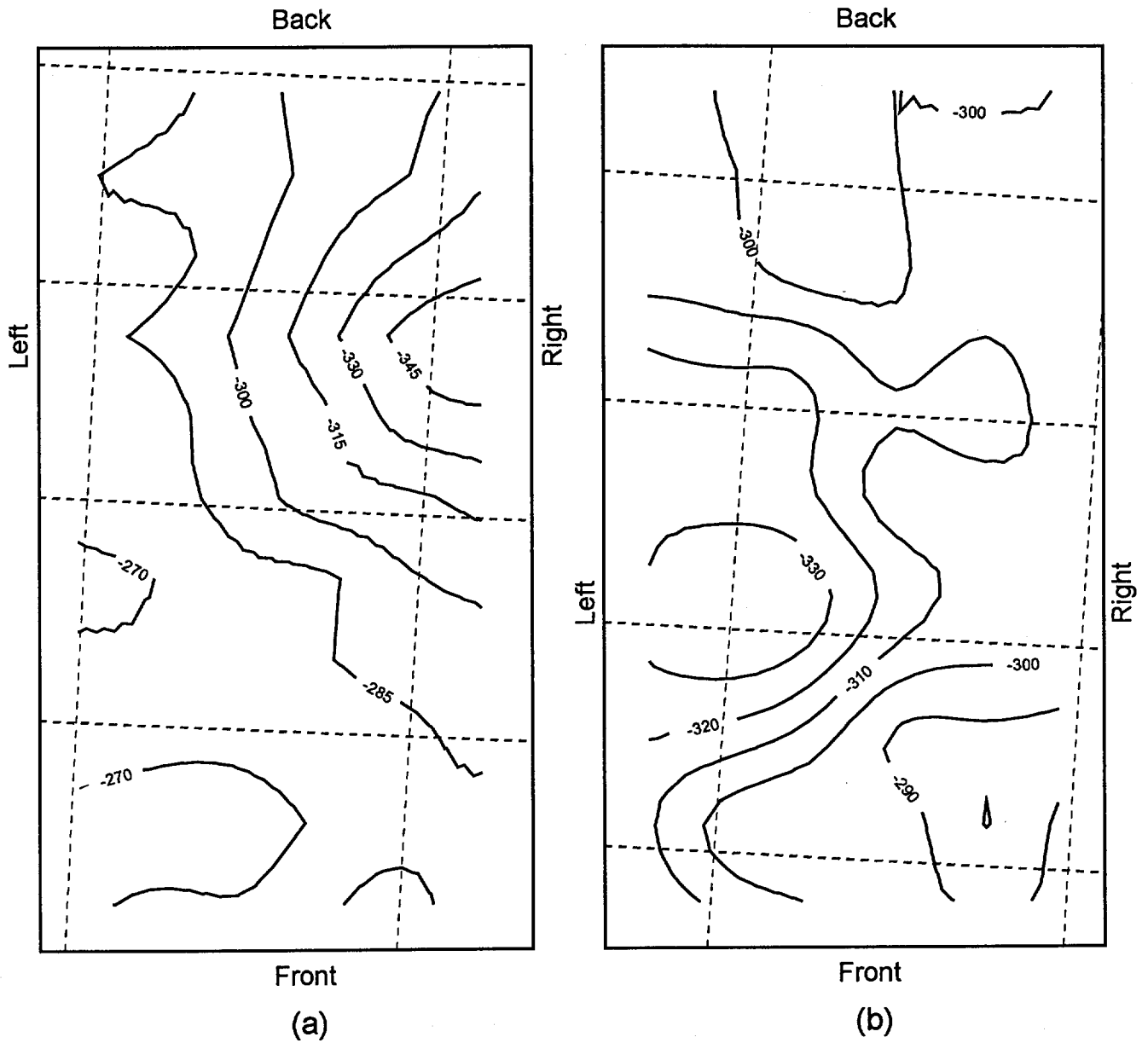a) set A (near the end of the wet cycle), and b) set B.

Figure 7. Potential mapping obtained after 9 days in the 21st. dry cycle for specimens :
a) F1A and b) F2A . The equipotential lines are drawn inside a scaled plan view of the dam
footprint. The labels (front, back, left and right) in the border of each map are given to define
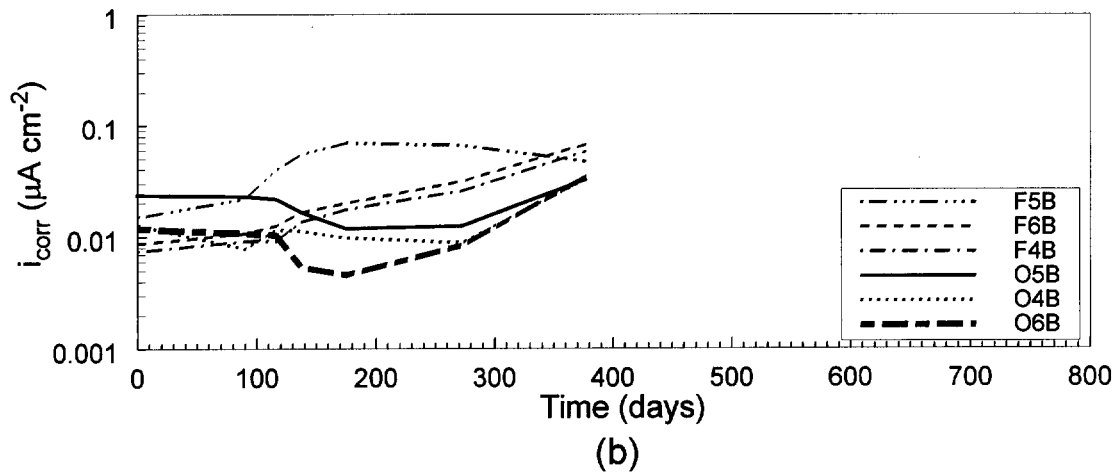the orientation of the specimens, according to Figure 1. Potentials vs. SCE.
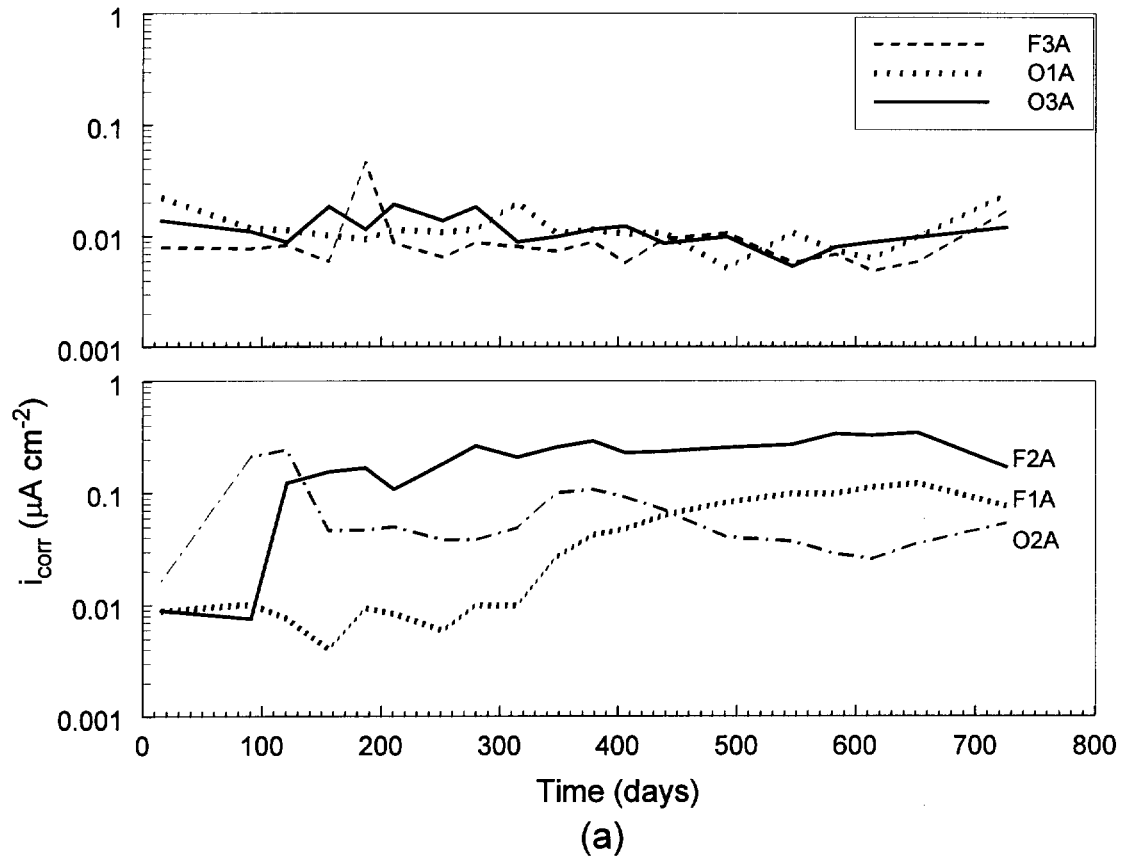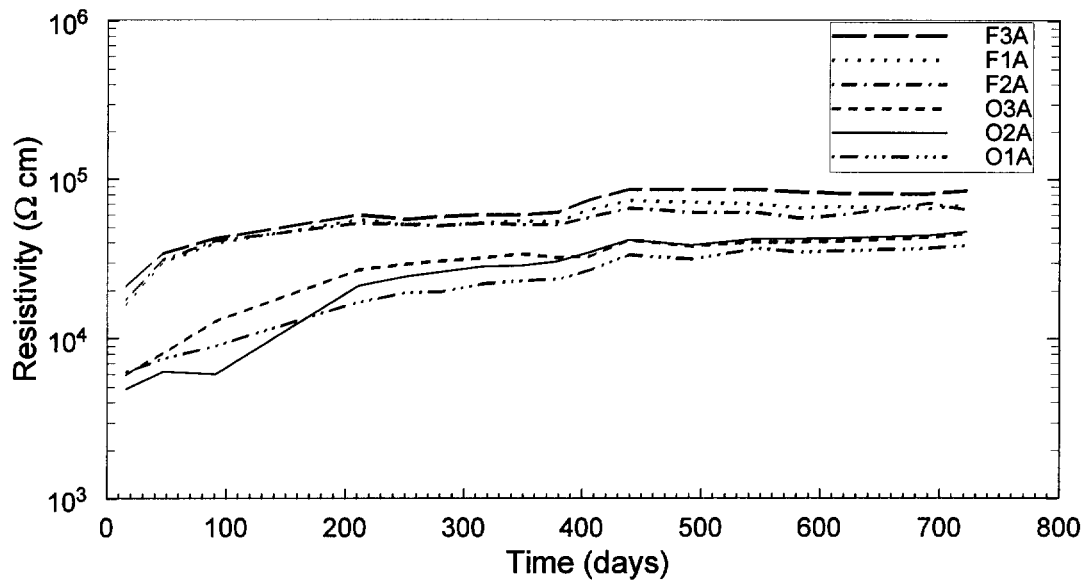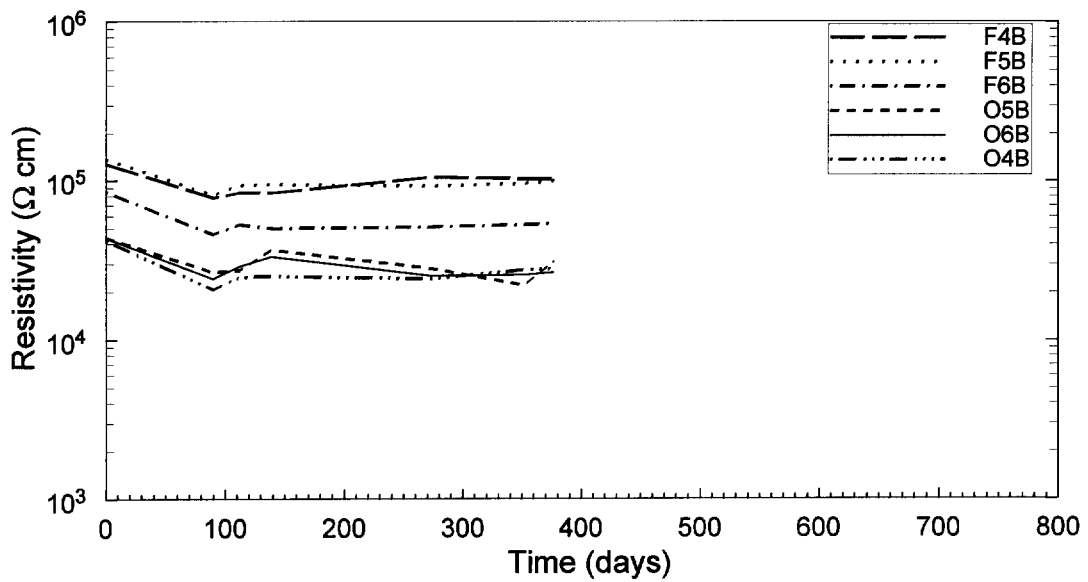
Figure 8. Evolution of nominal corrosion current density as a function of exposure time for specimens of : a) set A (near the end of the wet cycle) and b) set B.

Figure 9. Evolution of concrete resistivity as a function of time for specimens of:
a) set A (during the wet cycles) and b) set B (permanently wet, with
8 months fresh water preconditioning before day 0).